

# **Appendix 3: Cabo Ortegal Sample Collection**

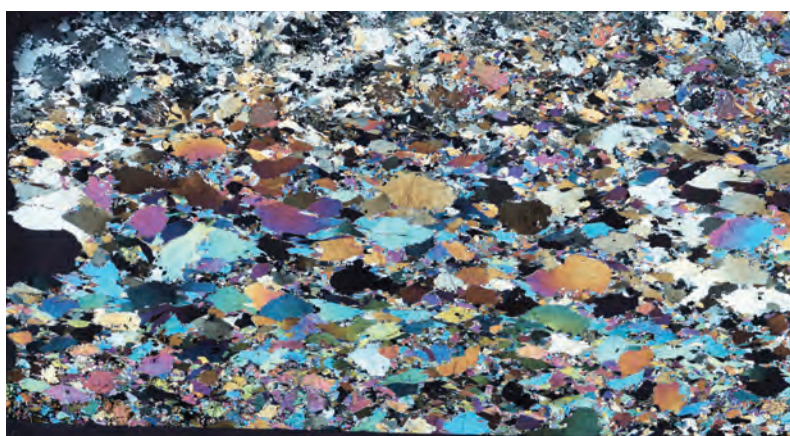
Note: All thin sections and drawings of block location on the sample are 27x46 mm.

CO67A

**Lithology:** Pyroxenite



**Minerals:** Opx, cpx, amphibole, sulfide



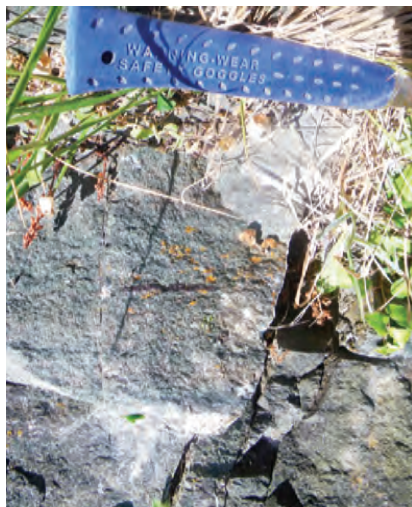
**Texture:** Changes across the section

**Observations:** Type-3 pyroxenite,  
Bands of large euhedral amphiboles  
visible between two sections that  
are more porphyroclastic



CO67B

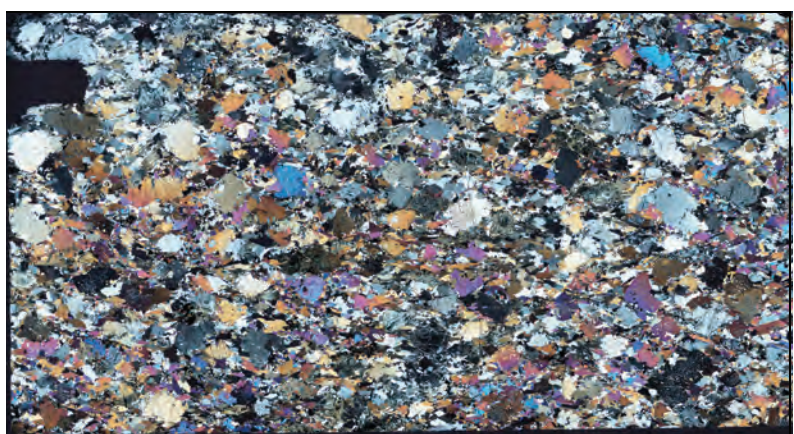
Lithology: Pyroxenite



Minerals: Opx, cpx, amphibole, sulfide

**Texture:** Porphyroclastic but can look equigranular in some parts

**Observations:** Type-3 pyroxenite  
The growth of amphibole gives an impression of a more equilibrated texture for pyroxenes than what it is



**CO96AA**

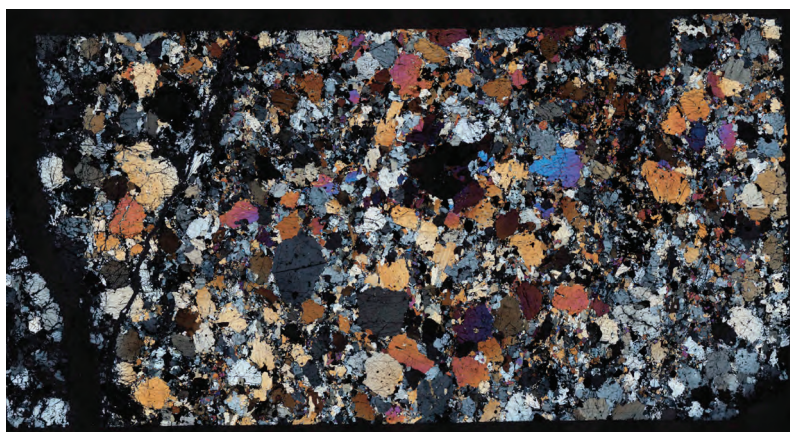
**Lithology:** Pyroxenite



**Minerals:** Opx, cpx, olivine, amphibole  
spinel, sulfide

**Texture:** Porphyroclastic

**Observations:** Type-1 pyroxenite,  
very clear porphyroclastic texture



CO96AB

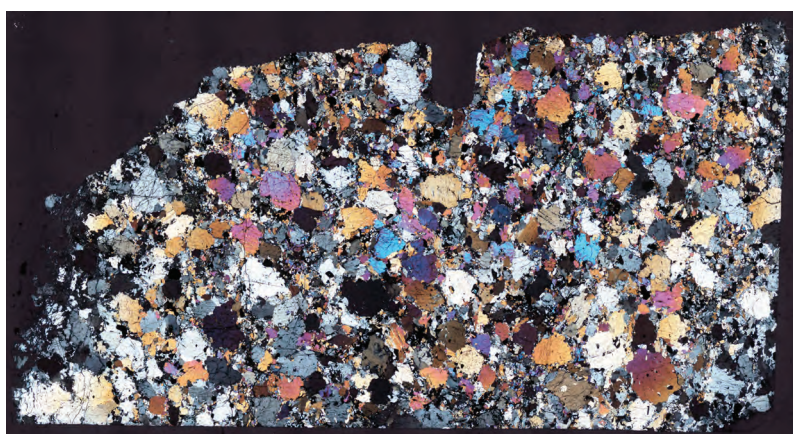
**Lithology:** pyroxenite



**Minerals:** opx, cpx, olivine, amphibole  
spinel, sulfide

**Texture:** Porphyroclastic

**Observations:** Type-1 pyroxenite



**C097A**

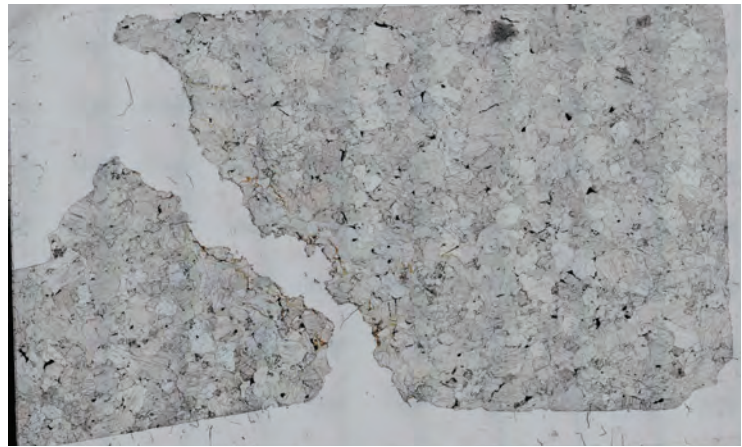
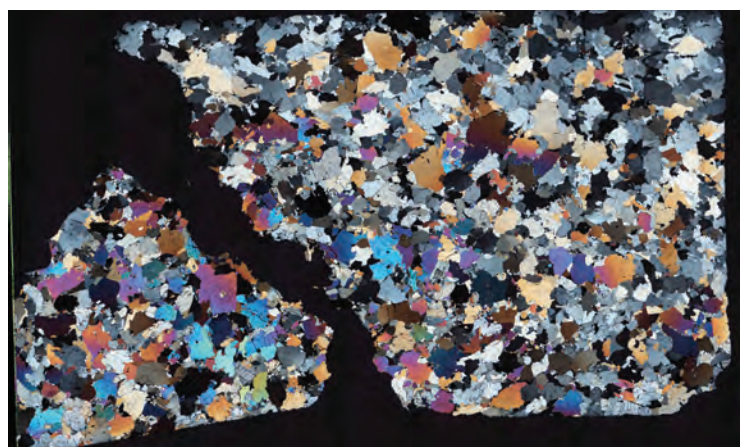
**Lithology:** Pyroxenite



**Minerals:** Opx, cpx, amphibole, spinel, sulfide

**Texture:** Porphyroclastic

**Observations:** Type-2 pyroxenite,  
The bimodal size distribution is not as  
strong as in other samples



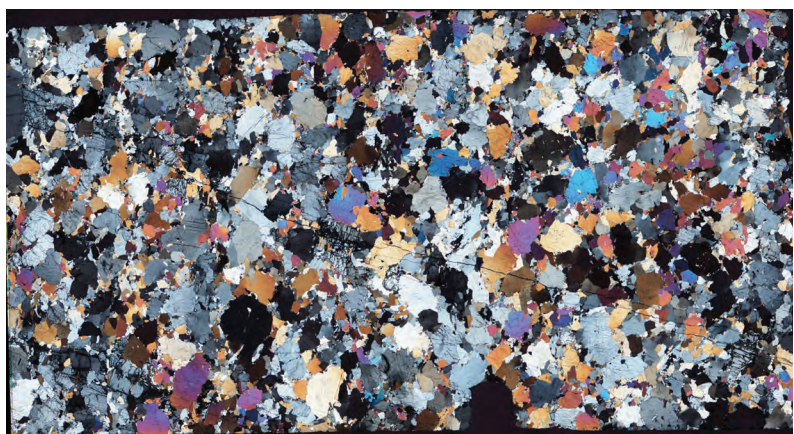
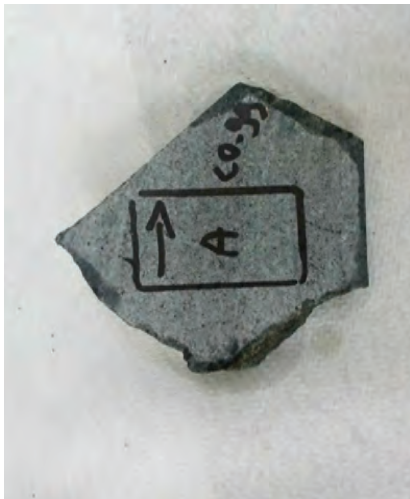
C099A

**Lithology:** Pyroxenite

**Minerals:** Opx, cpx, amphibole, spinel, sulfide

**Texture:** Porphyroclastic

**Observations:** Type-2 pyroxenite



CO100A

**Lithology:** Pyroxenite



**Minerals:** Opx, cpx, olivine, spinel, amphibole, sulfide

**Texture:** Porphyroclastic

**Observations:** Type-1 pyroxenite olivine-rich horizons are clearly visible thanks to the late serpentine overprint



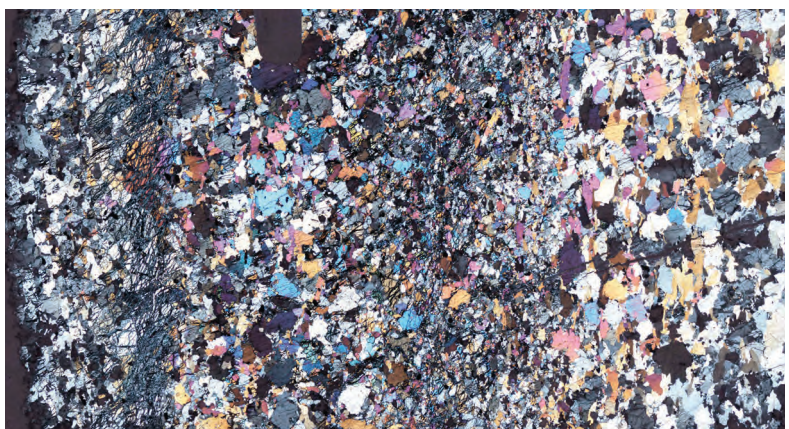
CO100B

**Lithology:** Pyroxenite

**Minerals:** Opx, cpx, olivine, spinel, amphibole, sulfide

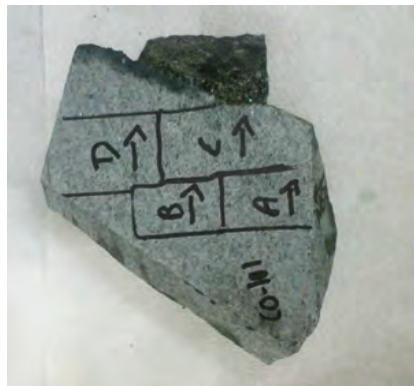
**Texture:** Porphyroclastic

**Observations:** Type- 1 pyroxenite, olivine-rich horizons are very visible



CO101C

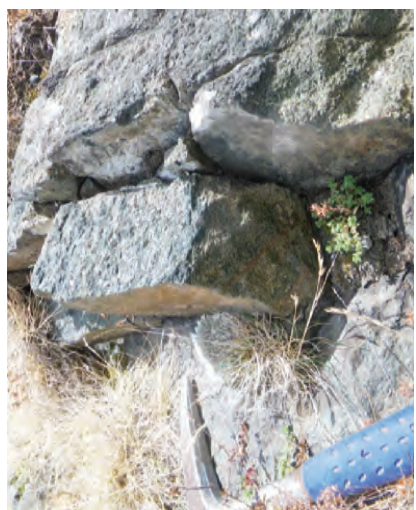
Lithology: Pyroxenite



Minerals: Opx, cpx, amphibole, sulfide

Texture: Equigranular

Observations: Type-3 pyroxenite  
Texture looks equilibrated because of  
the amphibole growth



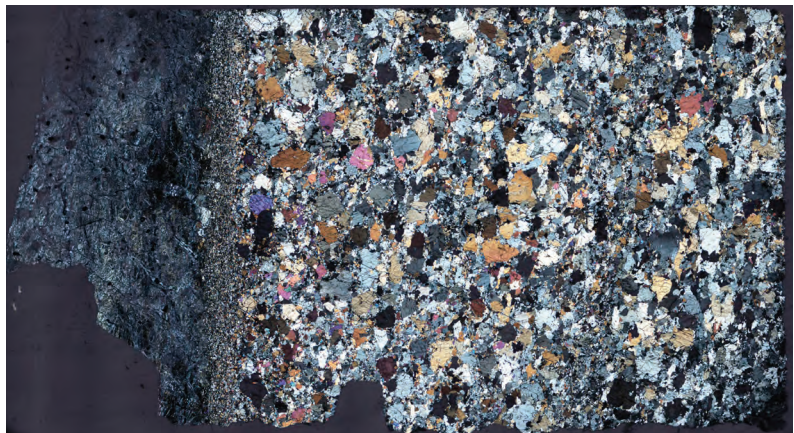
401A

**Lithology:** Pyroxenite

**Minerals:** Opx, cpx, olivine, amphibole, spinel, sulfide

**Texture:** Porphyroclastic

**Observations:** Type-1 pyroxenite  
Visible grain size reduction at the contact with the host dunite (top)



602C

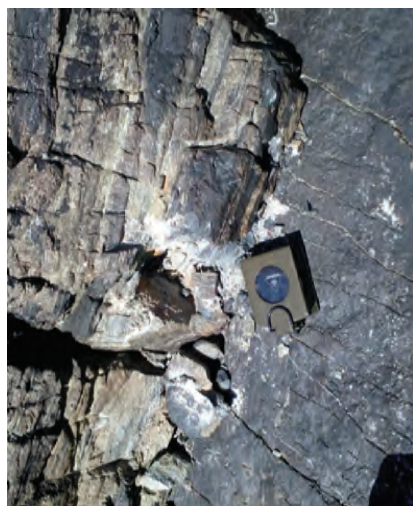
**Lithology:** Orthopyroxenite



**Minerals:** Opx, cpx, monticellite, amphibole, spinel, sulfide

**Texture:** Porphyroclastic

**Observations:** Type-4 pyroxenite Better-preserved layer from that sample. Cross-cutting of serpentine veins through the pyroxenite are visible and indicate a stronger viscosity for the pyroxenite in the serpentine stability domain.



**701BA**

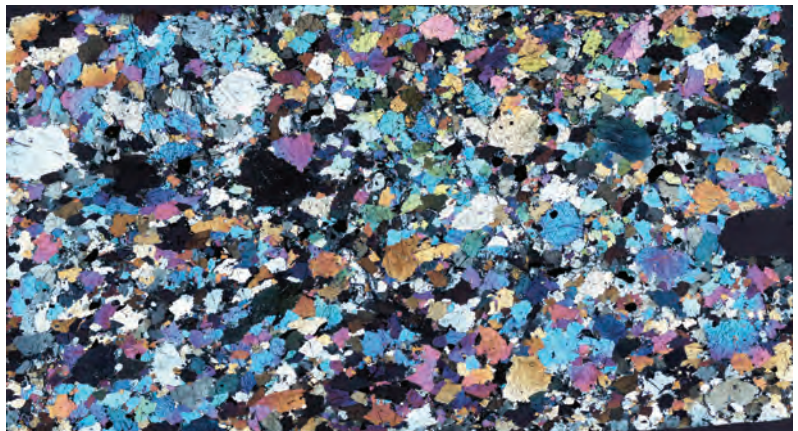
**Lithology:** Pyroxenite



**Minerals:** Opx, cpx, amphibole, spinel, sulfide, olivine

**Texture:** Granoblastic

**Observations:** Type-1 pyroxenite  
No olivine-rich layers are visible here  
but interstitial olivines are present



702A

**Lithology:** Pyroxenite

**Minerals:** Opx, cpx, olivine, amphibole  
spinel, sulfide

**Texture:** Porphyroclastic

**Observations:** Type-1 pyroxenite,  
with interstitial olivine in between  
pyroxenes



704A

**Lithology:** Orthopyroxenite

**Minerals:** Opx, olivine, cpx, amphibole,  
spinel, sulfide

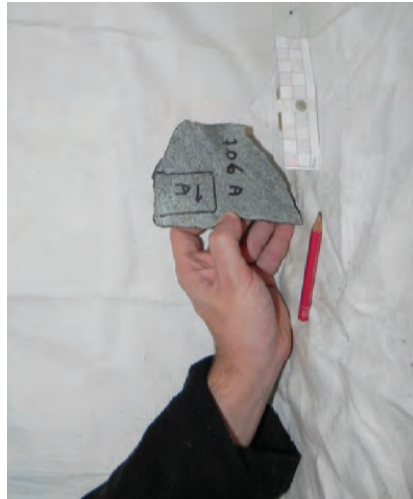
**Texture:** Porphyroclastic

**Observations:** Type-4 pyroxenite  
Layer thickness is decimetric



706AA

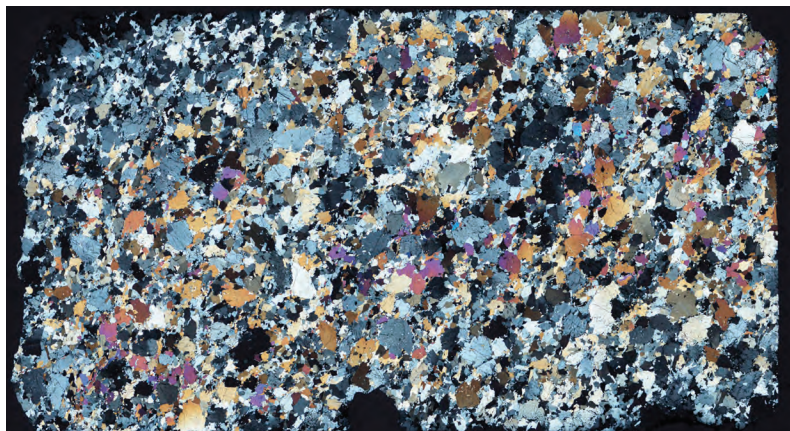
**Lithology:** Pyroxenite



**Minerals:** Opx, cpx, amphibole, spinel, sulfide

**Texture:** Porphyroclastic

**Observations:** Type-2 pyroxenite, most likely amongst the freshest samples collected







# **Appendix 4: Trinity Sample Collection**

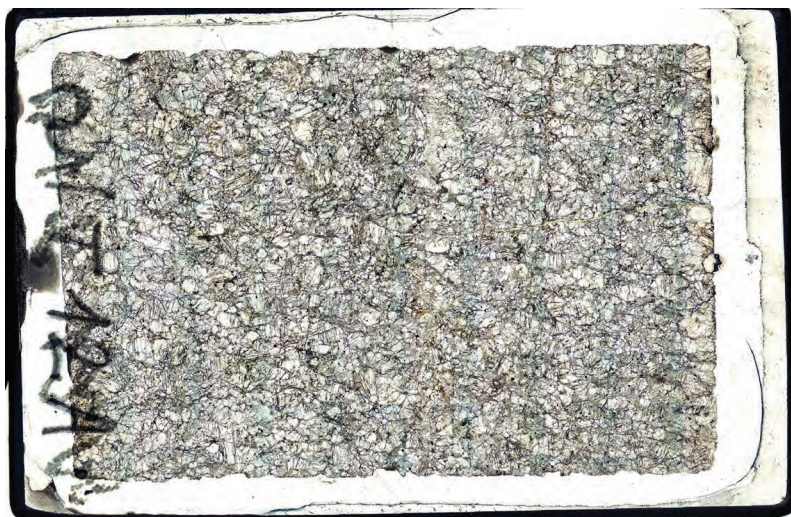
Note: All thin sections and drawings of block location on the sample are 27x46 mm.

**01T12A**

**Lithology:** Layered cumulates

**Minerals:** Olivine, opx, cpx, spinel,  
amphibole

**Texture:** Equilibrated equigranular

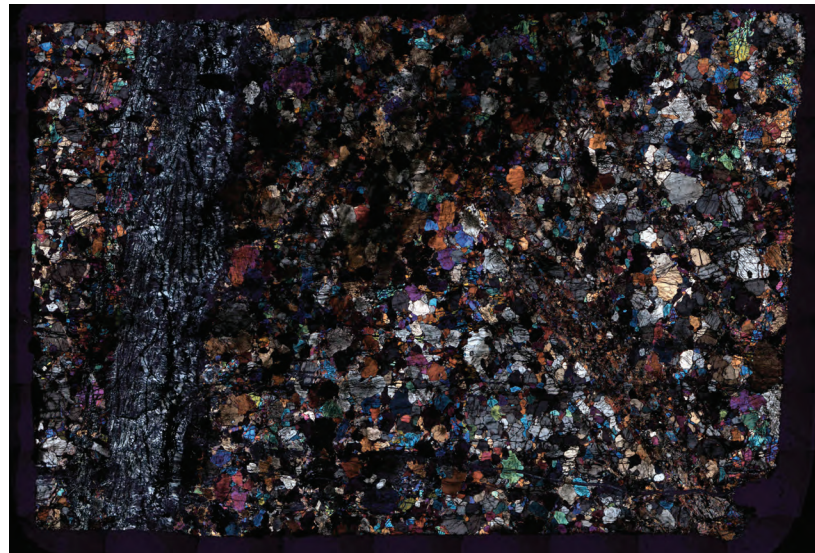


**01T13A**

**Lithology:** Layered cumulates

**Minerals:** Olivine, opx, cpx, spinel,  
amphibole

**Texture:** Equilibrated equigranular

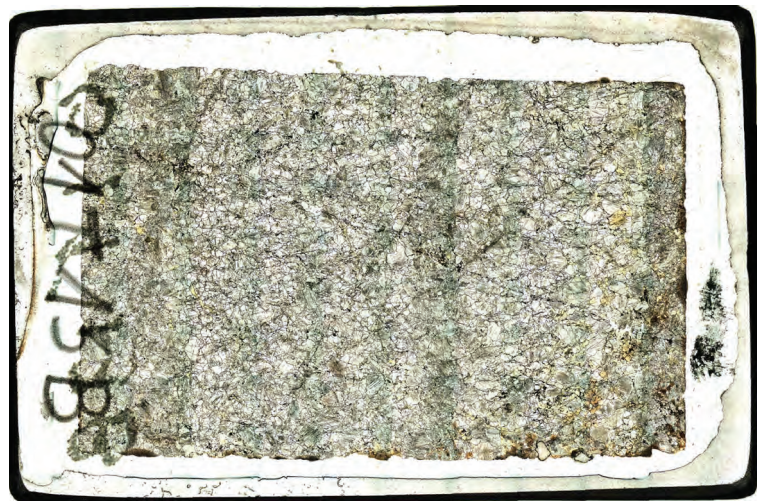


**01T13B**

**Lithology:** Layered cumulate

**Minerals:** Olivine, opx, cpx, spinel, amphibole

**Texture:** Equigranular and equilibrated



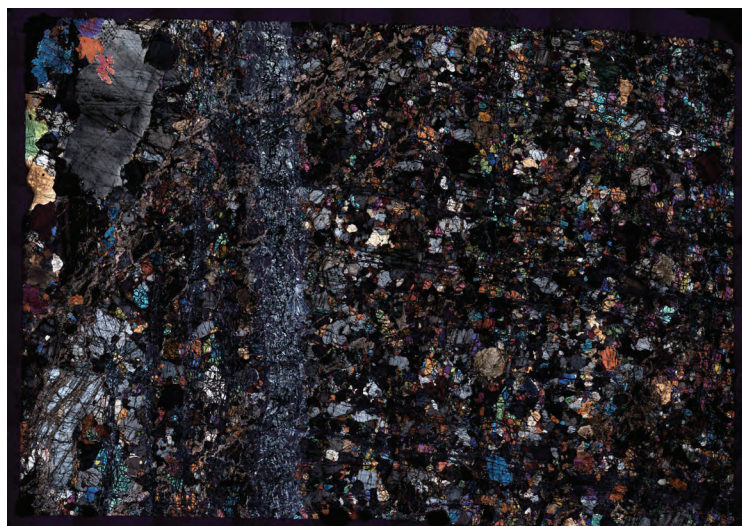
01T13C

**Lithology:** Layered cumulate

**Minerals:** Olivine, opx, cpx, spinel, amphibole

**Texture:** Equigranular and equilibrated

**Observations:** Finely layered cumulate in contact with coarser lithology at the top of the section



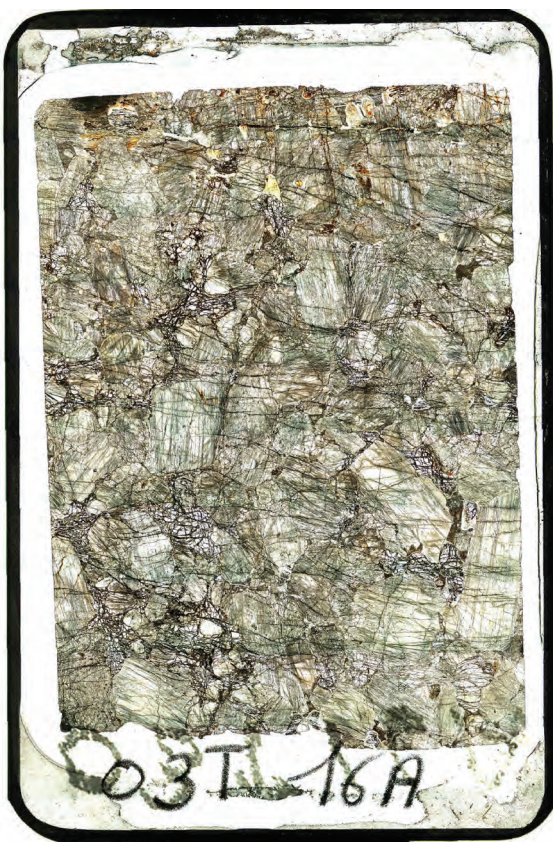
**03T16A**

**Lithology:** Pegmatite  
(i.e. coarse-grained fraction)

**Minerals:** Cpx, olivine, opx, amphibole

**Texture:** Coarse grained

**Observations:** Large euhedral grains  
of cpx associated with smaller cpx, opx  
and olivine matrix



03T46B

**Lithology:** Layered cumulate

**Minerals:** Olivine, opx, cpx, spinel, amphibole

**Texture:** Equigranular and equilibrated



17T4AA

**Lithology:** Dunite



**Minerals:** Olivine, spinel



**Texture:** Equilibrated equigranular

**Observations:** Foliation was invisible,  
lineation marked by spinel



17T4EA

Lithology: Lherzolite

Minerals: Olivine, opx, cpx, spinel

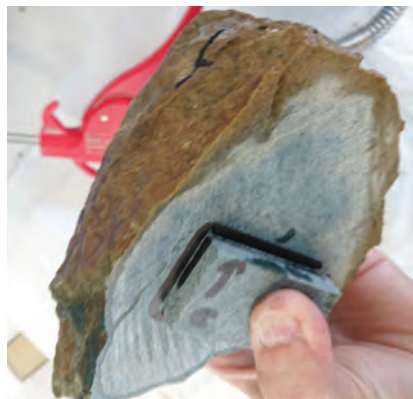
Texture: Equilibrated,  
bimodal grain size

Observations: Larger and smaller  
grains are located next to the  
pyroxene aggregates



17T25EA

**Lithology:** Dunite



**Minerals:** Olivine, spinel



**Texture:** Granoblastic

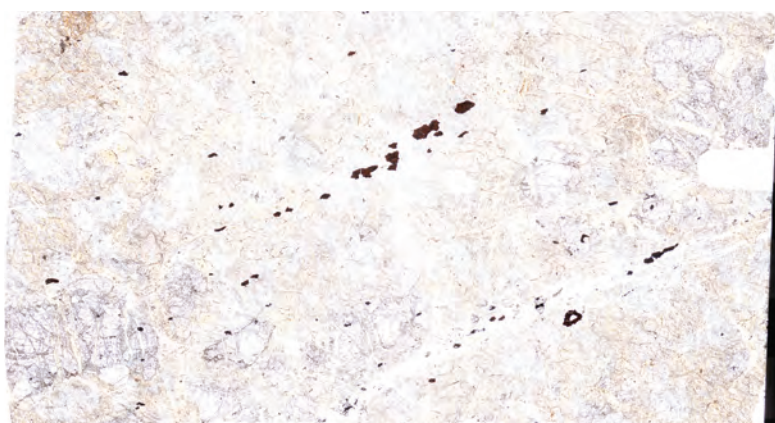
**Observations:** recrystallised texture  
close to textural equilibrium



**T1LD1A**

**Lithology:** Harzburgite

**Minerals:** Olivine, opx, spinel



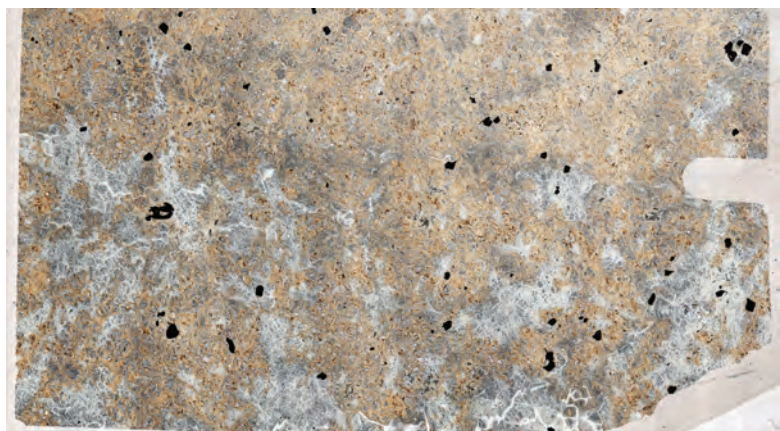
**T1LD2A**

**Lithology:** Dunite

**Minerals:** Olivine, spinel

**Texture:** Coarse-grained and  
equilibrated

**Observations:** Strong serpentisation,  
only lineation is visible.



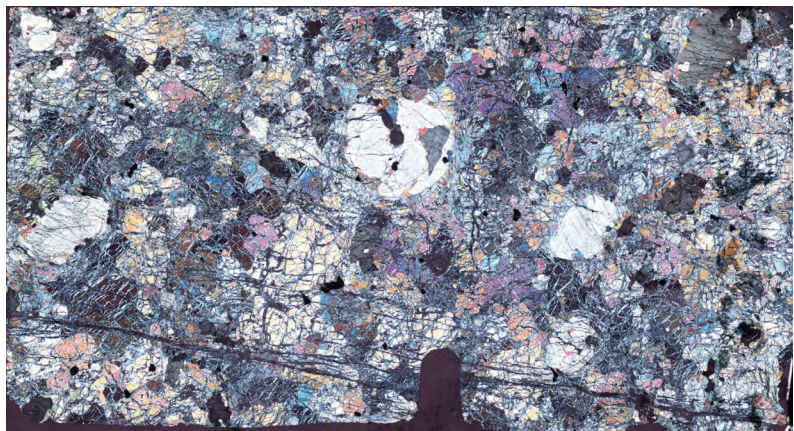
T2VB3A

**Lithology:** Lherzolite

**Minerals:** Olivine, opx, cpx, spinel, amphibole

**Texture:** Equilibrated with bimodal grain-size distribution

**Observations:** Structural framework unclear



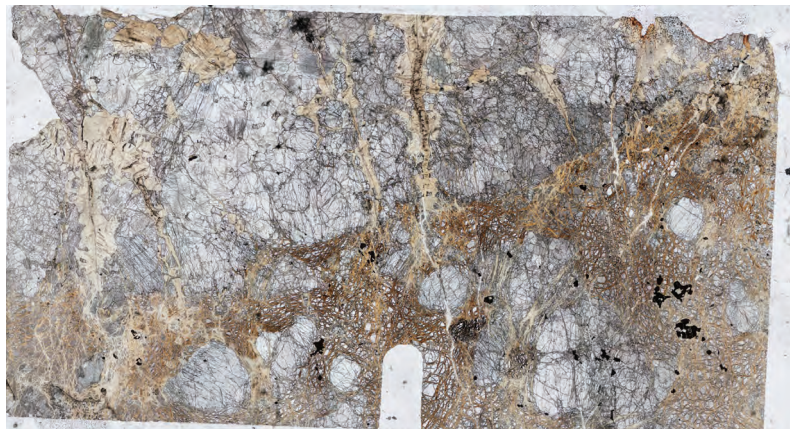
**T2VB4B**

**Lithology:** Lherzolite and pyroxenite

**Minerals:** Opx, cpx, olivine, spinel, amphibole

**Texture:** Equilibrated and close to equigranular

**Observations:** Texture is equigranular in both lherzolite and pyroxenite



**T3BC1A**

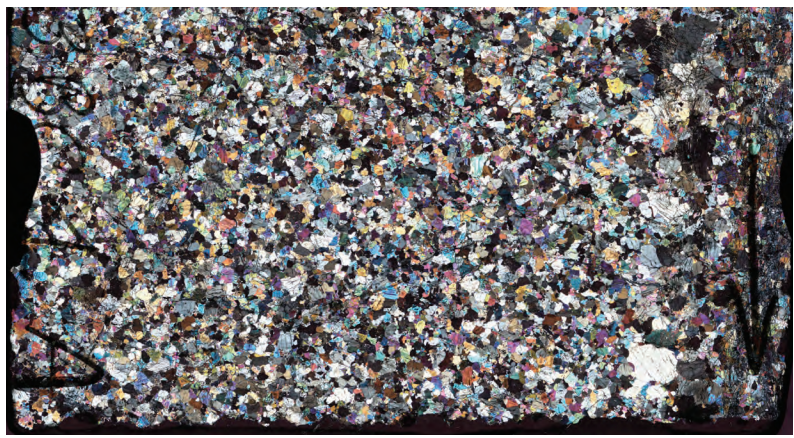
**Lithology:** Layered cumulates



**Minerals:** Opx, cpx, olivine, amphibole, spinel

**Texture:** Equigranular equilibrated

**Observations:** Layered cumulates, lineation not visible



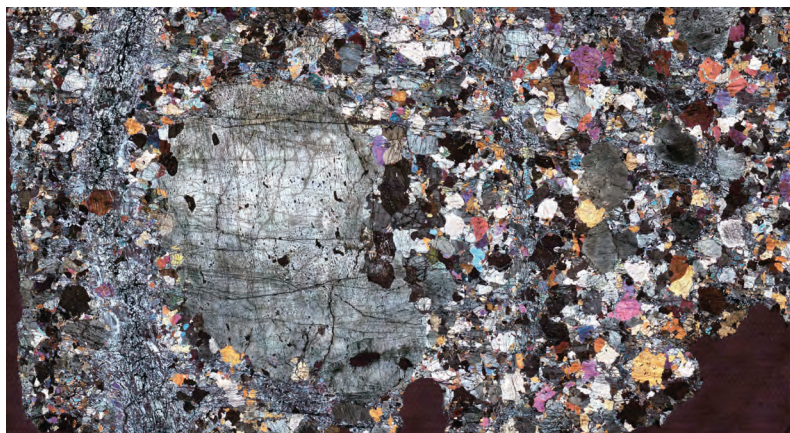
T3BC3A

**Lithology:** Pyroxenite

**Minerals:** Opx, cpx, amphibole,  
olivine, spinel

**Texture:** Equigranular and  
equilibrated

**Observations:** Macrocryst of opx  
perturbing the layering



**T3BC4A**

**Lithology:** Massive pyroxenite

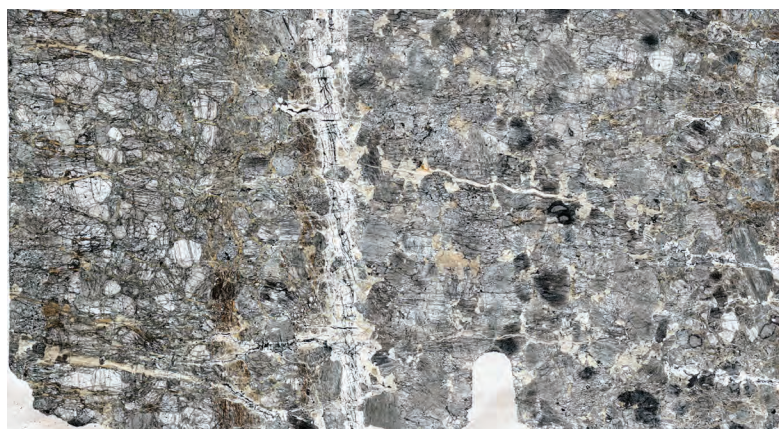
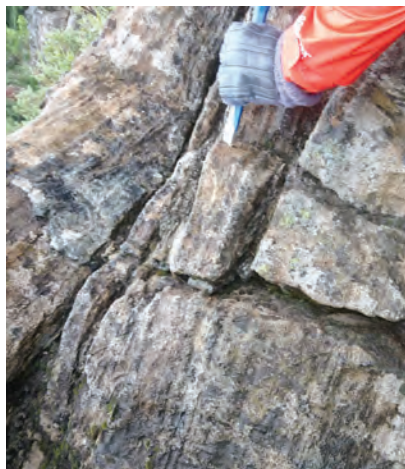


**Minerals:** Cpx, olivine, spinel



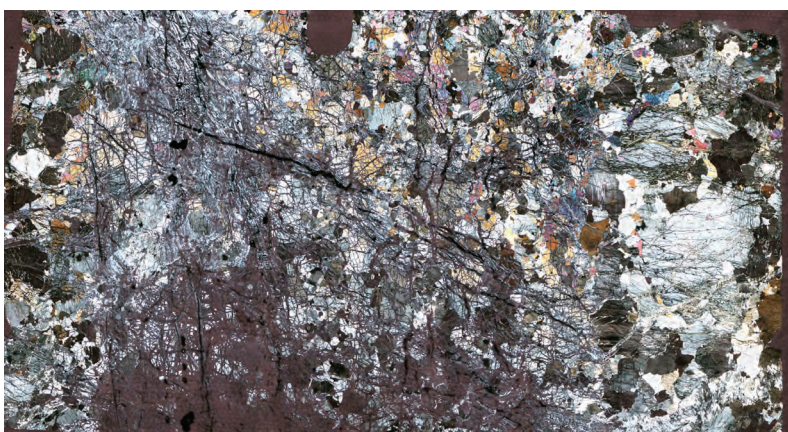
**Texture:** Unequilibrated with a  
bimodal grain distribution

**Observations:** olivine-rich layers  
are rarely visible on the field



**T4BC2A**

**Lithology:** Lherzolite and pyroxenite



**T4BC3A**

**Lithology:** Lherzolite

**Minerals:** Opx, cpx, olivine, spinel

**Texture:** Porphyroclastic

**Observations:** Strongly serpentinised,  
2 vertical meters below the layered  
cumulates



T4BC4A

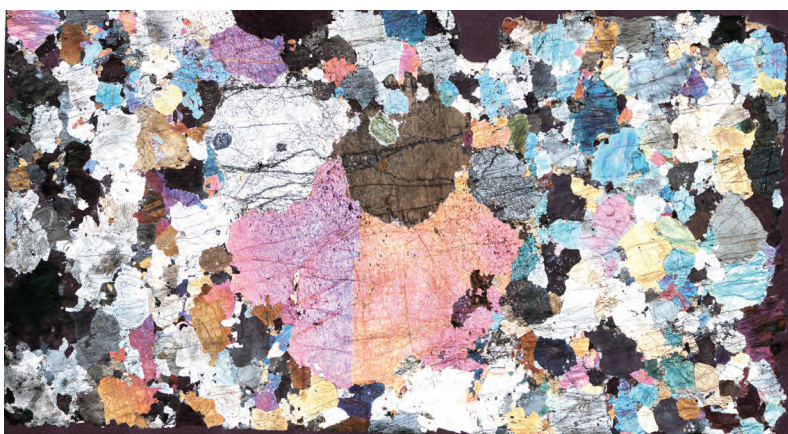
**Lithology:** Massive Pyroxenite



**Minerals:** Cpx, amphibole

**Texture:** Unequilibrated with  
bimodal grain size

**Observations:** Large twinned cpx,  
close to T3BC4A



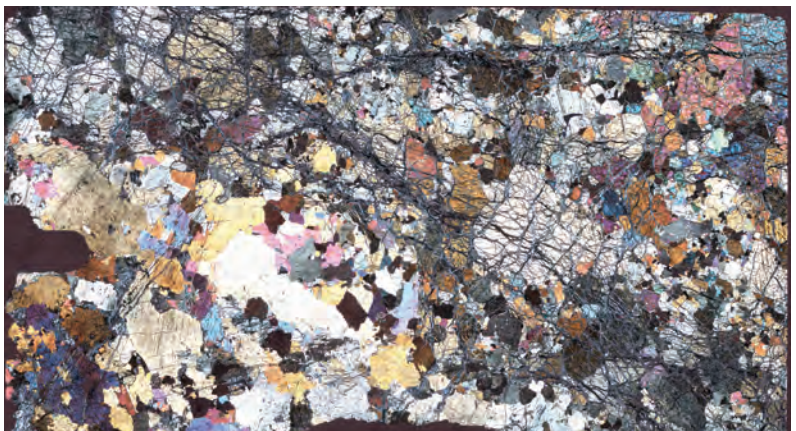
T4BC6A

**Lithology:** Peridotite and pyroxenite

**Minerals:** Olivine, cpx, opx, amphibole,  
spinel

**Texture:** Equilibrated with  
bimodal distribution

**Observations:** Peridotite xenolith  
in massive pyroxenites



T4BC7B

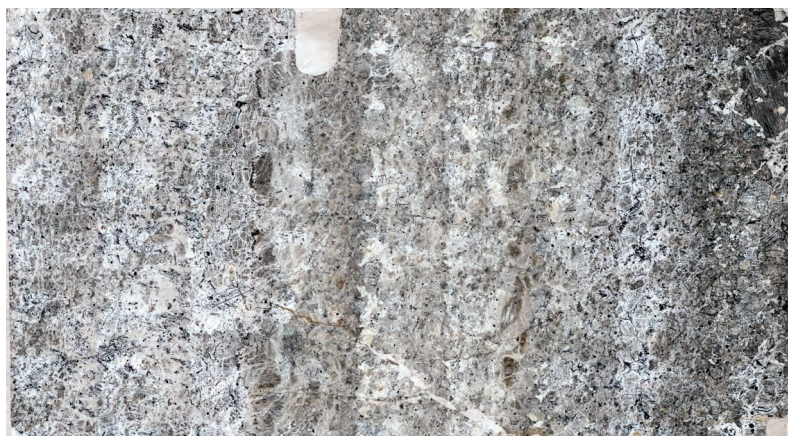
Lithology: Websterite



Minerals: Olivine, cpx, opx, spinel  
amphibole

Texture: Porphyroclastic

Observations: Last outcrop of  
cross-section for layered cumulates,  
strongly serpentинised



T4BC8A

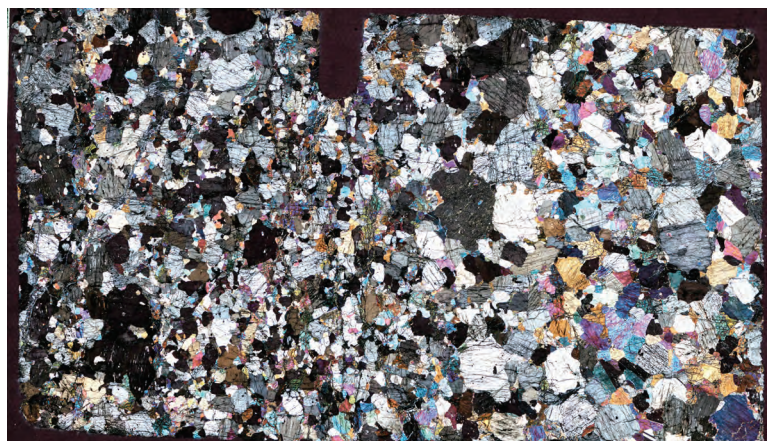
**Lithology:** Layered cumulates



**Minerals:** Olivine, opx, cpx, spinel, amphibole

**Texture:** Equilibrated equigranular

**Observations:** Tilted bending, a few hundred meters away from the main cross section



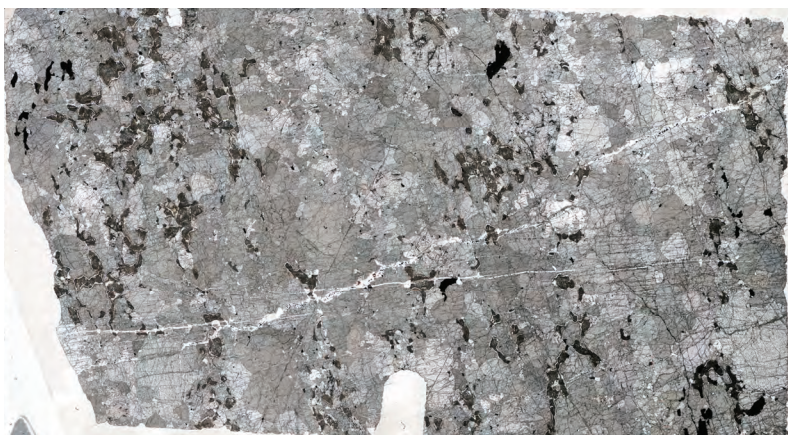
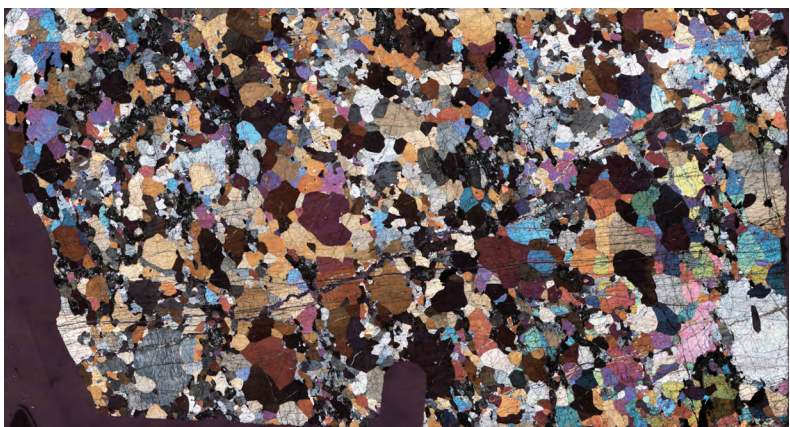
T5CP1A

**Lithology:** Lherzolite

**Minerals:** Olivine, cpx, opx, spinel,  
plagioclase

**Texture:** Equilibrated equigranular

**Observations:** Plagioclase-bearing  
Lherzolite with strong deformation  
visible in the field



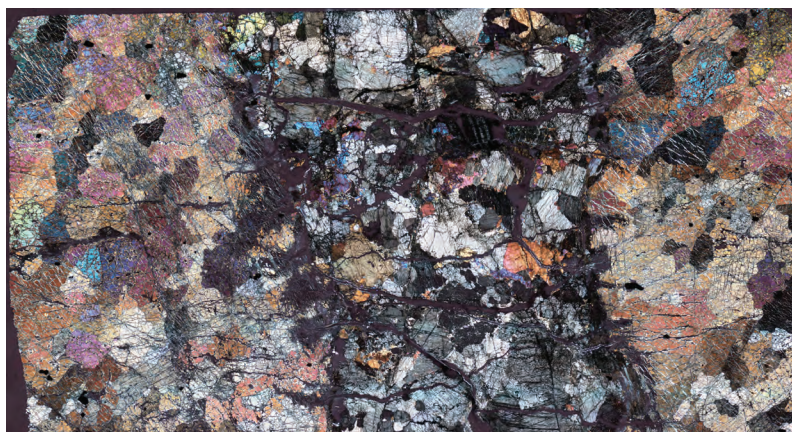
T5CP2A

**Lithology:** Dunite and pyroxenite

**Minerals:** Olivine, cpx, opx, amphibole, spinel

**Texture:** Equilibrated equigranular

**Observations:** Pyroxenite level in dunite. Dunite texture is equilibrated and equigranular. Pyroxenite texture has a more bimodal grain size distribution.





# Appendix 5: Publications

Direct output from the thesis:

**Henry, H.**, Tilhac, R., Griffin, W.L., O'Reilly, S.Y., Satsukawa, T., Kaczmarek, M.-A., Grégoire, M., Ceuleneer, G., 2017. [Deformation of mantle pyroxenites provides clues to geodynamic processes in subduction zones: Case study of the Cabo Ortegal Complex, Spain.](#) **Earth and Planetary Science Letters** 472, 174-185.

Collaboration relevant to the Cabo Ortegal pyroxenites:

Tilhac, R., Ceuleneer, G., Griffin, W.L., O'Reilly, S.Y., Pearson, N.J., Benoit, M., **Henry, H.**, Girardeau, J., Grégoire, M., 2016. [Primitive Arc Magmatism and Delamination: Petrology and Geochemistry of Pyroxenites from the Cabo Ortegal Complex, Spain.](#) **Journal of Petrology** 57, 1921-1954.

Tilhac, R., Grégoire, M., O'Reilly, S.Y., Griffin, W.L., **Henry, H.**, Ceuleneer, G., 2017. [Sources and timing of pyroxenite formation in the sub-arc mantle: Case study of the Cabo Ortegal Complex, Spain.](#) **Earth and Planetary Science Letters** 474, 490-502.

Collaboration on other ultramafic domains, EBSD analysis, data processing with Matlab and microstructure interpretations:

Xiong, Q., **Henry, H.**, Griffin, W. L., Zheng, J.-P., Satsukawa, T., Pearson, N. J., and O'Reilly, S. Y., 2017, [High- and low-Cr chromitite and dunite in a Tibetan ophiolite: evolution from mature subduction system to incipient forearc in the Neo-Tethyan Ocean: Contributions to Mineralogy and Petrology](#), v. 172, no. 6.



## Deformation of mantle pyroxenites provides clues to geodynamic processes in subduction zones: Case study of the Cabo Ortegal Complex, Spain



Hadrien Henry<sup>a,b,\*</sup>, Romain Tilhac<sup>a,b</sup>, William L. Griffin<sup>a</sup>, Suzanne Y. O'Reilly<sup>a</sup>, Takako Satsukawa<sup>a,c</sup>, Mary-Alix Kaczmarek<sup>d,b</sup>, Michel Grégoire<sup>a,b</sup>, Georges Ceuleneer<sup>b</sup>

<sup>a</sup> Australian Research Council Centre of Excellence for Core to Crust Fluid Systems (CCFS)/GEMOC, Department of Earth and Planetary Sciences, Macquarie University, Sydney NSW 2109, Australia

<sup>b</sup> Géosciences Environnement Toulouse (GET), CNRS, CNES, IRD, Université Toulouse III, 14 avenue E. Belin, 31400 Toulouse, France

<sup>c</sup> Department of Geophysics, Division of Earth and Planetary Sciences, Kyoto University, Kyoto 606-8502, Japan

<sup>d</sup> Institute for Earth Sciences (ISE), University of Lausanne, UNIL Moudon, Géopolis, 1015 Lausanne, Switzerland

### ARTICLE INFO

#### Article history:

Received 21 February 2017

Received in revised form 13 May 2017

Accepted 16 May 2017

Available online xxxx

Editor: J. Brodholt

#### Keywords:

mantle pyroxenites microstructure  
enstatite  
diopside  
supra subduction processes  
subduction conduit  
MTex

### ABSTRACT

In the Herbeira massif, Cabo Ortegal Complex, Spain, a well exposed assemblage of deformed dunites and pyroxenites offers a unique opportunity to investigate key upper mantle tectonic processes. Four types of pyroxenites are recognized: clinopyroxenites with enclosed dunitic lenses (type-1), massive websterites (type-2), foliated and commonly highly amphibolitized clinopyroxenites (type-3) and orthopyroxenites (type-4). Field and petrological observations together with EBSD analysis provide new insights on the physical behavior of the pyroxenes and their conditions of deformation and reveal the unexpected journey of the Cabo Ortegal pyroxenites.

We show that, during deformation, type-1 pyroxenites, due to their enclosed dunitic lenses, are more likely to localize the deformation than types-2 and -4 pyroxenites and may latter act as preferred pathway for fluid/melt percolation, eventually resulting in type-3 pyroxenites. All pyroxenite types display a similar response to deformation. Orthopyroxene deformed mostly by dislocation creep; it shows kink bands and undulose extinction and its fabric is dominated by [001]||100. Clinopyroxene displays subgrain rotation, dynamic recrystallization and fabric with [010] axes clustering next to the foliation pole and [001] axes clustering next to the lineation suggesting activation of [001]||110 and [001]||100 in some samples. These observations are in good agreement with deformation at temperatures greater than 1000 °C. Olivine in type-1 and type-4 pyroxenites shows [100]||010 or [001]||010 fabrics that are consistent with deformation at temperatures >1000 °C and may indicate deformation in a hydrous environment. The amphibole [001]||100 fabric gives insights on a lower-temperature deformation episode (~800 to 500 °C). Our results, interpreted in the light of published experimental data, together with the regional geological and geochemical studies are consistent with the following tectonic evolution of the Cabo Ortegal pyroxenites: (1) delamination from an arc root in a mantle-wedge setting at temperatures above 1000 °C and (2) introduction into a relatively softer subduction channel where deformation was accommodated by localized shear zones, thus preserving the high-temperature fabrics of pyroxenites. The Cabo Ortegal pyroxenites may therefore be seen as a rare exposure of deformed mantle-wedge material.

© 2017 Elsevier B.V. All rights reserved.

### 1. Introduction

Rheological models of the upper mantle traditionally adopt a major assumption: the physical properties of mantle peridotites

can be satisfactorily inferred from those of olivine. This working hypothesis is being challenged by studies highlighting the potentially important volume of pyroxenes, in the shallow upper mantle and from the transition zone to the crust. Evenly-distributed pyroxenes may modify the bulk rheological properties of peridotites, compared to an unrealistic assemblage of pure olivine, and partly condition their behavior during penetrative deformation. On the other hand, local concentrations of pyroxenes (e.g. layering) may influence the distribution of deformation and lead *inter alia* to

\* Corresponding author at: Australian Research Council Centre of Excellence for Core to Crust Fluid Systems (CCFS)/GEMOC, Department of Earth and Planetary Sciences, Macquarie University, Sydney NSW 2109, Australia.

E-mail address: hadrien.henry@mr.edu.au (H. Henry).



## Sources and timing of pyroxenite formation in the sub-arc mantle: Case study of the Cabo Ortegal Complex, Spain



Romain Tilhac<sup>a,b,\*</sup>, Michel Grégoire<sup>a,b</sup>, Suzanne Y. O'Reilly<sup>a</sup>, William L. Griffin<sup>a</sup>, Hadrien Henry<sup>a,b</sup>, Georges Ceuleneer<sup>b</sup>

<sup>a</sup> ARC Centre of Excellence for Core to Crust Fluid Systems (CCFS) and GEMOC, Department of Earth and Planetary Sciences, Macquarie University, Sydney NSW 2109, Australia

<sup>b</sup> Géosciences Environnement Toulouse (GET), Université de Toulouse, CNRS, IRD, 14 avenue E. Belin, 31400 Toulouse, France

### ARTICLE INFO

#### Article history:

Received 23 December 2016

Received in revised form 7 July 2017

Accepted 7 July 2017

Available online 27 July 2017

Editor: F. Moynier

#### Keywords:

north-western Iberia

Variscan suture

Herbiera massif

mantle websterite

radiogenic isotopes

REE diffusion timescale

### ABSTRACT

Pyroxenites exposed in ophiolites and orogenic peridotite massifs may record petrogenetic processes occurring in mantle domains generated and/or transferred in supra-subduction environments. However, the timing of their formation and the geochemical characteristics of their source region commonly are obscured by metamorphic and metasomatic overprints. This is especially critical in arc-related environments, where pyroxenites may be formed during the differentiation of primitive magmas. Our approach combines Sr- and Nd-isotope geochemistry and geochronology, and modelling of REE diffusion, to further constrain the origin of a well-characterized set of pyroxenites from the arc-related Cabo Ortegal Complex, Spain. In the light of petrological constraints, Sr- and Nd-isotope systematics consistently indicate that cpx and amphibole have acquired disequilibrium during two main episodes: (1) a magmatic/metamorphic episode that led to the formation of the pyroxenites, coeval with that of Cabo Ortegal granulites and corresponding to the incipient stage of a potential Cadomian arc (459–762 Ma; isochron and second-stage Nd model ages); (2) an episode of metamorphic amphibolitization upon the percolation of relatively unradioactive and LREE-enriched hydrous fluids, subsequent to the delamination of the pyroxenites from their arc-root settings during Devonian subduction. Calculations of diffusional timescale for the re-equilibration of REE are consistent with this scenario but provide only poor additional constraints due to the sensitivity of this method to grain size and sub-solidus temperature. We thus emphasize the necessity to combine isochron ages and Nd model ages corrected for radiogenic ingrowth to put time constraints on the formation of subduction-and/or collision-related pyroxenites, along with petrological and geochemical constraints. Homogeneous age-corrected  $^{143}\text{Nd}/^{144}\text{Nd}$  of 0.5121–0.5125 ( $\epsilon_{\text{Nd}}$ ) between 0 and +7.5 and  $^{87}\text{Sr}/^{86}\text{Sr}$  of 0.7037–0.7048 provide information on the sources of the metasomatic agents involved (and potentially the parental melts) and notably indicate the contributions from enriched mantle components (EM I and/or II). This suggests the involvement of an old crustal component, which is consistent with the derivation of the pyroxenites and granulites from an ensialic island arc, potentially built on the northern margin of either Gondwana or a pre-Gondwanan continental block. This case study thus documents the role of melt–rock reactions as major pyroxenite-forming processes in the sub-arc mantle, providing further constraints on their sources and timing in the Cabo Ortegal Complex.

© 2017 Elsevier B.V. All rights reserved.

### 1. Introduction

The mineralogical and geochemical diversity of pyroxenites observed in peridotite massifs and xenoliths provides a unique record of the petrological processes contributing to the evolution of lithospheric mantle domains (Downes, 2007, for a review).

Despite their minor abundance, their geodynamic significance is strengthened by their implication in the petrogenesis and transfer of mantle-derived magmas in various tectonic environments (e.g. Sobolev et al., 2007). Different types of mantle pyroxenites have been reported, representing crystallized products of *in-situ* partial melting or metamorphic segregations of peridotites (e.g. Dick and Sinton, 1979), metamorphosed products of recycled oceanic lithosphere (Allègre and Turcotte, 1986) and high-pressure crystal cumulates from migrating mantle melts (e.g. Bodinier et al., 1987). Studies of exhumed mantle terranes, such as Ronda (Spain),

\* Corresponding author at: ARC Centre of Excellence for Core to Crust Fluid Systems (CCFS) and GEMOC, Department of Earth and Planetary Sciences, Macquarie University, Sydney NSW 2109, Australia.

E-mail address: romain.tilhac@mq.edu.au (R. Tilhac).

## Primitive Arc Magmatism and Delamination: Petrology and Geochemistry of Pyroxenites from the Cabo Ortegal Complex, Spain

Romain Tilhac<sup>1,2\*</sup>, Georges Ceuleneer<sup>2</sup>, William L. Griffin<sup>1</sup>,  
Suzanne Y. O'Reilly<sup>1</sup>, Norman J. Pearson<sup>1</sup>, Mathieu Benoit<sup>2</sup>,  
Hadrien Henry<sup>1,2</sup>, Jacques Girardeau<sup>3</sup> and Michel Grégoire<sup>1,2</sup>

<sup>1</sup>Australian Research Council Centre of Excellence for Core to Crust Fluid Systems (CCFS) and GEMOC, Department of Earth and Planetary Sciences, Macquarie University, Sydney, NSW 2109, Australia; <sup>2</sup>Géosciences Environnement Toulouse (GET), Observatoire Midi Pyrénées, Université de Toulouse, CNRS, IRD, 14 avenue E. Belin, 31400 Toulouse, France; <sup>3</sup>Laboratoire de Planétologie et Géodynamique de Nantes (LPGN), Université de Nantes, CNRS, 2 rue de la Houssinière, 44322 Nantes Cedex 3, France

\*Corresponding author. E-mail: romain.tilhac@mq.edu.au

Received October 28, 2015; Accepted September 28, 2016

### ABSTRACT

The genesis of primitive arc magmas has had a major impact on continent formation through time, but the rarity of exposures of deep arc sections limits our understanding of the details of melt migration and differentiation. Abundant pyroxenites are exposed within a 600 m thick section of arc-related mantle harzburgites and dunites in the Herbeira massif of the Cabo Ortegal Complex, Spain. We report a combination of field and petrographic observations with *in situ* and whole-rock geochemical studies of these pyroxenites. After constraining the effects of secondary processes (serpentinitization, fluid or melt percolation and amphibolitization), we determine that the low Al content of pyroxenes, high abundance of compatible elements and the absence of plagioclase reflect melt–peridotite interaction and crystal segregation from primitive hydrous melts at relatively low pressure (<1.2 GPa). Olivine clinopyroxenites and olivine websterites preserving dunite lenses (type 1 and 3 pyroxenites) represent the products of partial replacement of peridotites at decreasing melt/rock ratio following the intrusion of picritic melts. Massive websterites (type 2) may represent the final products of this reaction at higher melt/rock ratios. They crystallized from more Si-rich (boninitic) melts, potentially generated through differentiation of the initially picritic melts or intruded as dykes and veins. Rare opx-rich websterites (type 4) were produced by interaction of these melts with dunites. Chromatographic re-equilibration accompanied late-magmatic crystallization of amphibole from migrating or trapped residual melts. This percolative fractional crystallization produced a range of rare earth element (REE) patterns from spoon-shaped in type 1 pyroxenites to strongly light REE (LREE)-enriched in type 2 and 3 pyroxenites. Particularly high CaO/Al<sub>2</sub>O<sub>3</sub> ratios (2.2–11.3) and the selective enrichment of large ion lithophile elements (LILE) over high field strength elements (HFSE) in Cabo Ortegal pyroxenites suggest the generation of Ca-rich picritic–boninitic parental melts via low-degree, second-stage melting of a refractory Iherzolite at <2 GPa, following percolation of slab-derived fluids and/or carbonatite melts. Pyroxenites and their host peridotites record high-temperature deformation followed by the development of sheath folds and mylonites. Peak metamorphism was then reached under eclogite-facies conditions (1.6–1.8 GPa and 780–800 °C) as recorded by undeformed garnet coronas around spinel. We suggest that this episode corresponds to the delamination of an arc root owing to gravitational instabilities arising from the presence of abundant pyroxenites within mantle harzburgites. Retrograde metamorphism and hydration under amphibolite-facies conditions were recorded by abundant post-kinematic amphibole, which corresponds to the exhumation of the arc root after its intrusion into a subduction zone. The Cabo Ortegal Complex thus preserves

## High- and low-Cr chromitite and dunite in a Tibetan ophiolite: evolution from mature subduction system to incipient forearc in the Neo-Tethyan Ocean

Qing Xiong<sup>1,2</sup> · Hadrien Henry<sup>1,3</sup> · William L. Griffin<sup>1</sup> · Jian-Ping Zheng<sup>2</sup> ·  
Takako Satsukawa<sup>4</sup> · Norman J. Pearson<sup>1</sup> · Suzanne Y. O'Reilly<sup>1</sup>

Received: 8 February 2017 / Accepted: 21 April 2017 / Published online: 23 May 2017  
© Springer-Verlag Berlin Heidelberg 2017

**Abstract** The microstructures, major- and trace-element compositions of minerals and electron backscattered diffraction (EBSD) maps of high- and low-Cr# [spinel Cr# = Cr<sup>3+</sup>/(Cr<sup>3+</sup> + Al<sup>3+</sup>)] chromitites and dunites from the Zedang ophiolite in the Yarlung Zangbo Suture (South Tibet) have been used to reveal their genesis and the related geodynamic processes in the Neo-Tethyan Ocean. The high-Cr# (0.77–0.80) chromitites (with or without diopside exsolution) have chromite compositions consistent with initial crystallization by interaction between boninitic magmas, harzburgite and reaction-produced magmas in a shallow, mature mantle wedge. Some high-Cr# chromitites show crystal-plastic deformation and grain growth on previous chromite relics that have exsolved needles of diopside. These features are similar to those of

the Luobusa high-Cr# chromitites, possibly recycled from the deep upper mantle in a mature subduction system. In contrast, mineralogical, chemical and EBSD features of the Zedang low-Cr# (0.49–0.67) chromitites and dunites and the silicate inclusions in chromite indicate that they formed by rapid interaction between forearc basaltic magmas (MORB-like but with rare subduction input) and the Zedang harzburgites in a dynamically extended, incipient forearc lithosphere. The evidence implies that the high-Cr# chromitites were produced or emplaced in an earlier mature arc (possibly Jurassic), while the low-Cr# associations formed in an incipient forearc during the initiation of a new episode of Neo-Tethyan subduction at ~130–120 Ma. This two-episode subduction model can provide a new explanation for the coexistence of high- and low-Cr# chromitites in the same volume of ophiolitic mantle.

Communicated by Othmar Müntener.

**Electronic supplementary material** The online version of this article (doi:10.1007/s00410-017-1364-y) contains supplementary material, which is available to authorized users.

✉ Qing Xiong  
qing.xiong@mq.edu.au

<sup>1</sup> Department of Earth and Planetary Sciences, ARC Centre of Excellence for Core to Crust Fluid Systems (CCFS) and GEMOC, Macquarie University, Sydney, NSW 2109, Australia

<sup>2</sup> State Key Laboratory of Geological Processes and Mineral Resources, School of Earth Sciences, China University of Geosciences, Wuhan 430074, China

<sup>3</sup> Géosciences Environnement Toulouse (GET), Université de Toulouse, CNRS, IRD, 14 Avenue E. Belin, Toulouse 31400, France

<sup>4</sup> Division of Earth and Planetary Sciences, Department of Geophysics, Kyoto University, Kyoto 606-8502, Japan

**Keywords** High- and low-Cr chromitite and dunite · Tibetan ophiolites · Compositions and microstructures of chromitites · Melt–peridotite interaction · Subduction episodes in Neo-Tethyan Ocean

### Introduction

The composition of chromite in ophiolitic chromitites and associated dunites is sensitive to the nature of reactant magmas and peridotites, and hence can be used to track tectonic environments and melt–peridotite (including melt–melt) interaction in the upper mantle (e.g., Dick and Bullen 1984; Arai 1992; Zhou and Robinson 1997; Barnes and Roeder 2001; Kamenetsky et al. 2001; Rollinson 2008; Gonzalez-Jimenez et al. 2011, 2014; Arai and Miura 2016). However, the coexistence of high- and low-Cr# [spinel Cr# = atomic Cr<sup>3+</sup>/(Cr<sup>3+</sup> + Al<sup>3+</sup>)] chromitites with

